3D Geomechanical Modeling of Complex Salt Structures

Wouter van der Zee[1], Cem Ozan[2], Martin Brudy[2], Marc Holland[3]

[1]Baker Hughes - Reservoir Development Services, Lange Kleiweg 50c, 2288GK, Rijswijk, the Netherlands.
[2]Baker Hughes - Reservoir Development Services, 5373 West Alabama Str., Suite 300, Houston, TX 77056, USA.
[3]Baker Hughes - Reservoir Development Services, Emmerich-Josef Str. 5, 55116, Mainz, Germany.

Abstract: Some of the most active and high profile hydrocarbon plays currently being explored and developed around the world lie below a salt canopy of variable depth, geometry, and thickness. Drilling through a thick salt canopy can provide a more effective way to reach a sub-salt objective rather than drilling through thick overpressured sediments in a supra-salt mini-basin. Unfortunately, wellbore stability problems, such as unexpected low fracture gradient, are relatively common while drilling close and out of these salt structures. Thus, significant drilling costs could be eliminated if these hazards could be identified and avoided in the well planning process.

In this paper, we present the workflow starting from the structural information through the FE mesh creation and population of its properties to the final 3D finite element based geomechanical modeling. The resulting 3D stress field around salt structures helps to significantly improve the wellbore stability predictions. The workflow described provides an efficient way to create realistic 3D finite-element simulations from complicated structural data. It is optimized for the best resolution around the area of interest (well trajectory) while limiting the size of the numerical problem to an order that can be handled in reasonable times. The workflow allows for a detailed simulation of the stress field around salt bodies that is new to the hydrocarbon industry and helps to significantly reduce the risk for wellbore failures of increasingly costly wells drilled to exploit, e.g. sub-salt plays in the Gulf of Mexico.

Keywords: Geomechanics, Wellbore Stability, Creep, Visualization.

1. Introduction

Many major exploration and new field development efforts around the world (i.e., Gulf of Mexico (GOM), Campos Basin (Brazil), Angola, West Africa) take place in near- or sub-salt fields where the salt canopies have variable depths, geometries, and thicknesses. Drilling through these thick salt canopies can provide a more effective way to reach the target reservoir rather than drilling through surrounding overpressured sediments. Unfortunately, wellbore stability problems, such as unexpected low fracture gradient, are relatively common while drilling through and out of these salt structures. Significant drilling costs could be eliminated if these hazards could be identified

and avoided in the well planning process. Since the in-situ stress and temperature fields are critical and major input parameters for wellbore stability prediction studies, it is of utmost importance to have a good understanding of the stress and the temperature fields near and within salt structures.

The most pronounced effect of a salt structure on the stress state is due to the fact that salt cannot sustain differential stresses and thus, creeps in response to any applied deviatoric stress. As a result, the stress state within a salt structure would be nearly isotropic (though not necessarily lithostatic [Fredrich et al., 2007]). This near isotropic stress state within the salt causes the principal stresses in the surrounding formation to re-orientate from their far field orientations to be almost parallel and perpendicular to the salt-formation interfaces. In other words, the principal stress orientations are not necessarily vertical and horizontal around salt structures. Moreover, the stress magnitudes in the formation are altered close to salt structures. The density differences between the salt and the surrounding formations also contribute to alterations in the stress magnitudes. In addition, the presences of salt canopies also alter the far- field temperature gradients around and within the salt structures. This is due to the fact that the thermal conductivity of salt is 2-3 times greater than that of surrounding formations. Thus, salt structures act as channels for heat transport and cause thermal anomalies around these canopies (Yu et al., 1992). This is particularly important if rate of wellbore closure within salt is of interest since the creep rate of salt strongly depends on temperature (Willson et al., 2003).

Utilizing 3D finite element models which can yield high resolution results along the path to be used in wellbore stability calculations significantly improves wellbore stability predictions. In this paper, we present the workflow established by Baker Hughes Reservoir Development Services (RDS) to efficiently develop such 3D finite element models. We also present an example case in which this workflow is utilized to understand and quantify how the presence of salt is perturbing the stress state.

2. Methods

The construction of the 3D geomechanical model of complex salt structures consists of the following steps with the workflow illustrated in Figure 1:

1. Define initial or undisturbed stress state
2. Build structural model
3. Build 3D property model
4. Build 3D finite element (FE) mesh
5. Populate 3D FE mesh with material properties
6. Obtain initial elastic equilibrium
7. Calculate perturbed stress state
8. Visualize and quality check results

In this workflow, the commercially available program JewelSuite (www.jewelsuite.com) together with Abaqus/CAE and ABAQUS/Standard is utilized as described later in the paper.

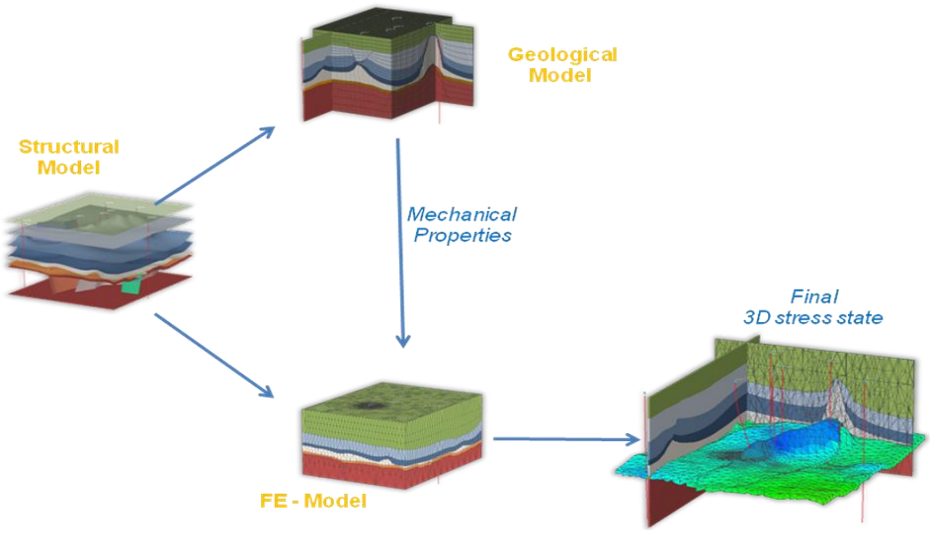

Figure 1: Workflow of building a 3D geomechanical model of complex salt structures.

2.1 Geomechanical Input

The purpose of the FE simulations discussed in this paper is to calculate the stress alterations caused by the presence of salt (i.e., creep) in the surroundings formations. These changes are restricted to a certain volume around an isolated salt body. Outside this volume, the influence of the salt body vanishes and the stresses approach the regional "back-ground" stress state. We call this regional, undisturbed stress field "the initial stress state" and use it in our FE model at the start of the simulations. In the case of an isolated salt body such as a salt dome or a salt wall, the "far-field stress state" can be derived from the analysis of wells sufficiently remote from the salt body. However, for the case of an allochthonous salt sheet as encountered in the Gulf of Mexico, it is almost impossible to find wells that are not drilled through salt and thus, are not influenced by the presence of salt.

The stress state consists of total vertical stress (S_v), maximum total horizontal stress (S_{Hmax}), minimum total horizontal stress (S_{hmin}), pore pressure (P_p), and azimuth of the maximum horizontal stress (Azi_{SH}). The stress state is derived by detailed analysis of logging data, drilling experience, and analysis of wellbore failures such as breakouts and drilling induced tensile fractures. A more detailed description of these workflows is given in Brudy et al. (1997) and Moos and Zoback (1990) and will only be summarized in this paper where it is necessary.

The overburden stress for the initial stress state is approximated by vertical integration of the available densities. The densities can originate from density wire line or LWD logs, or can be calculated from velocity data. The velocity data, in turn, can be derived from wire line or LWD logs, but can also be derived from 3D seismic: the so-called interval velocity. Interval velocities are normally available from 3D seismic processing to be used for the time-depth conversion process. It is of advantage to derive density from the seismic velocities since the 3D density cube

created as such reflects the natural variation of the velocities in vertical and lateral directions. To derive density from seismic interval velocities, traces of velocity data are extracted along calibration wells and a correlation between interval velocity and density is derived. Using this calibrated correlation, the 3D density volume is calculated from the 3D interval velocity volume.

The pore pressure is estimated using log-based pore pressure prediction methods (Bowers, 1994; Ward et al., 1992); however, if 3D interval velocities are available, the pore pressure is predicted using relevant methods as described in Bowers (1994) and Moos et al. (2004).

To derive a profile of the least principal stress S_{hmin}, (extended) leak-off or mini frac test results from calibration wells in the region are analyzed (Gaarenstrom et al., 1993; Raaen and Brudy, 2001). In the case of isolated salt bodies, data from calibration wells that are not influenced by the presence of salt are separated from wells that are close to the salt body. Figure 2 displays effective stress ratios derived from leak-off pressures from both groups of wells. The first group, the plot on the left side in Figure 2, is located close to the salt body and the second group, the plot on the right side in Figure 2, is sufficiently remote from the salt structure so that the leak-off pressure is not affected by the salt body. For every reliable leak-off pressure, the corresponding effective stress ratio (ESR also called K_0) is calculated using

$$ESR = \frac{S_{h\min} - P_p}{S_v - P_p} \qquad \text{Eq. 1}$$

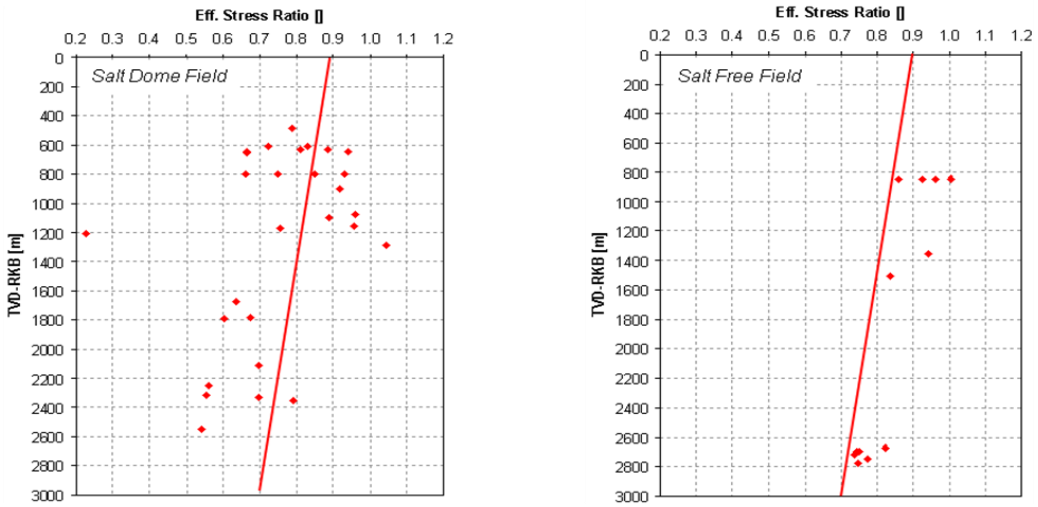

Figure 2: Effective stress ratio plots for fields affected (left) and not affected (right) by the presence of a salt structure.

Once the ESR data from the observation wells are compiled, a linear equation is fit to the ESR data in an ESR vs. TVD plot. This best fit line allows extrapolation of the leak-off test results to depths that are not covered by the leak-off tests and thus, will be used to calculate the horizontal stress profile in the model based on the vertical stress and pore pressure as given in Equation 1. In

our example case, clearly, two different trends are identified. The ESR trend derived from the wells remote to the salt body is used to define the S_{hmin} depth profile for the initial stress state and therefore, used to assign the starting stress state in the FE simulations.

The azimuth of the maximum horizontal stress is derived from image log or oriented caliper log analyses in which drilling induced wellbore failure, such as breakouts, or drilling induced tensile fractures are used to determine the azimuth of S_{Hmax}. The magnitude of S_{Hmax} is calculated using S_v, S_{hmin}, P_p, Azi_{SH} and the rock strength. A good review of these methods can be found in Zoback et al. (2003) and Zoback (2007).

2.2 3D Structural Model

The geological model and finite element mesh are based on structural depth information gathered through 3D seismic. The results of the seismic interpretation are obtained either as 3D point data described by easting, northing and depth coordinates or as polyline data described by the easting, northing and depth coordinates and connectivity of these points.

The first step in building the mesh is the construction of structural surfaces from the 3D point data or polyline data. For the cases shown in this article, the commercial available program JewelSuite was used to create the 3D surfaces. The constructed surfaces are compared with the formations tops available in the well data. A mismatch between well markers and the seismic data can be due to an error in the time-depth conversion, or due to an error in the seismic interpretation. This is especially the case when picking near salt structures due to the bad seismic data quality commonly found near salt structures. If the discrepancy between the seismic and the well data is not significant, the surfaces can be adjusted to the well markers to build a consistent model. If there is a considerable discrepancy, probably the seismic processing is invalid and has to be repeated.

An important part of the construction of a valid structural model is to honor all surface contacts. Especially when there are salt structures in the model as the case considered in this paper, this can be a cumbersome task due to the complex geometry of the contacts. Each surface has to have a perfect or "water-tight" contact, which means that no gaps are allowed at the intersections. The perfect fit between the surfaces is necessary to define a formation by an enclosed volume and to be able to apply material properties per formation in the finite element model.

In the previous step, the most geologically realistic surfaces are constructed; therefore, the meshing process attempts to honor these surfaces as closely as possible. These optimized 3D surfaces are meshed with fine triangles near curved structures, and with large triangles in the flat areas in order to minimize the amount of triangles required to describe the surface as detailed as possible. However, the characteristics of the FE mesh should be different: the FE mesh should be finely meshed in the volume of interest (e.g., along the well trajectory) to create smooth profiles of the final results, while, at the same time, the total number of elements has to be restricted to ensure that the numerical problem can be solved in a reasonable time. Therefore, the surfaces have to be re-meshed such that the final mesh would have a fine mesh around the well path or structure of interest and gets courser at the outer. The re-meshing algorithm, built-in within the geomechanics workflow in JewelSuite, consists of two parts. In the first part, an area is defined on a surface which is not to be re-meshed but stored. This is the area of interest which stays unchanged during re-meshing. In part two, the rest of the surface around the area of interest is re-meshed such that the triangles on the new mesh get courser as they get closer to the outer boundaries. The re-meshing algorithm makes sure that each node in the new mesh is on the original surface. As a

result, re-meshing yields a mesh with low density of nodes at the outside borders, and denser near the area of interest. The quality of the triangles is optimized to be able to generate a high-quality FE mesh. All contacts between the different surfaces are honored, to keep the valid geometry intact (Figure 3).

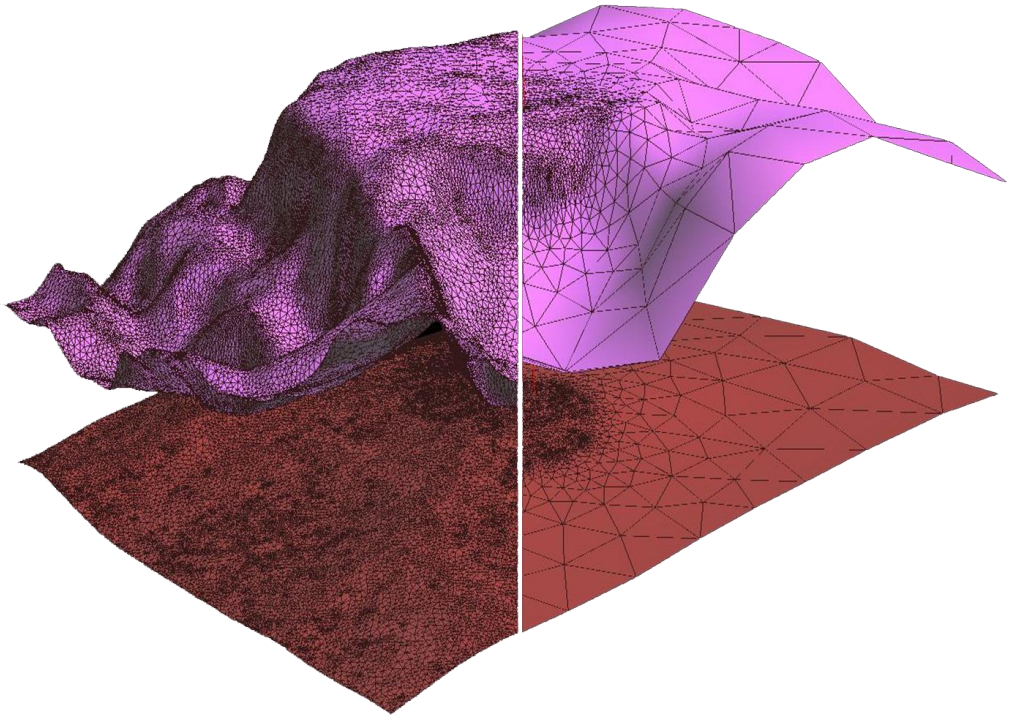

Figure 3: Re-meshing of triangulated horizons. The original surface (left) is re-triangulated to obtain a gradient from coarse triangles on the outside to fine triangles at the center (right).

2.3 Mechanical properties

An important step in the creation of a realistic 3D geomechanical model is the definition of the mechanical properties as a function of formation and position. We use statistical methods for extrapolation of well information guided by seismic information (using, for example, Kriging algorithms) to create 3D cubes of the mechanical material properties. These methods are commonly used in oil industry especially in reservoir characterization studies.

In the 3D model, the mechanical properties describing rock behavior have to be determined. In the finite element model, two different constitutive laws are used: salt is modeled as a power-law creep material with no internal pore pressure; all other (clastic) rocks are modeled as poro-elastic materials for which an internal pore pressure is defined and deformations are governed by effective stresses.

The deformation behavior of poro-elastic materials is characterized by Young's modulus and Poisson's ratio. The Young's modulus is calculated from the sonic and density data as given in equation 2. Preferably, this is done using compressional wave velocity (V_p) and shear wave velocity (V_s). If the latter is not available it can be calculated from V_p using the Castagna mudrock equation as given in equation 3 below (Castagna, 1985).

$$E_{dyn} = \rho V_s^2 \cdot \frac{3V_p^2 - 4V_s^2}{V_p^2 - V_s^2} \qquad \text{Eq. 2}$$

$$V_s = 0.862 \cdot V_p - 1.172 \qquad \text{Eq. 3}$$

where V_p and V_s are in km/sec.

The dynamic calculated Young's modulus is converted to a static modulus either using a field-specific conversion or a general factor.

The behavior of the salt is described by a standard power-law creep model for pure halite. Possible variations of the creep behavior dependent on the position within the salt body and caused by temperature, composition, or impurities are neglected for the FE simulations.

Since the wellbore stability prediction is the main goal of the FE simulations, an unconfined compressive strength (UCS) profile is also derived from seismic interval velocities. If rock mechanical laboratory tests are available in the calibration wells, these tests are used to calibrate the empirical equation linking interval velocity to UCS. In most cases, however, rock mechanical tests are not available for most of the overburden. Thus, a consistency check between the observed wellbore failure in the calibration wells and the failure predicted using this rock strength (UCS) is carried out for calibration purposes.

2.4 3D FE mesh generation

The next step is converting the structural model, which consists only of surfaces, into a solid model. This process is started within JewelSuite. The actual 3D mesh building is performed in Abaqus/CAE using a proprietary Python script. The automated process is as follows:

- The remeshed triangulated surfaces are exported from JewelSuite in a so-called tsurf format, an ascii format commonly used for these kind of objects.
- The Python script converts this format into a CAD format which can be imported into Abaqus/CAE as shells.
- The shells are merged to one part, including lateral and bottom surfaces.
- In the next step, this part is converted to a solid using the shells-to-solid conversion operation.
- The scripts define sets and add material property classes to all cells in the model.
- The boundary conditions are defined for the whole model including water load on top of the model.
- An input file is written out which is used to import the solid structure back into JewelSuite.

The solid model is meshed with 2nd order tetrahedrons. Two types of elements are used for the meshing: elements with the pore pressure degree of freedom (C3D10MP) used for modeling the

clastic sediments, and elements without the pore pressure degree of freedom (C3D10M) used for modeling the salt. The sizes of the solid elements are controlled in the same manner as the surface triangles to generate a solid mesh which is fine in the area of interest, and coarse to the outside boundaries (Figure 4). In the several examples in this paper total amount of elements are limited to ~450,000.

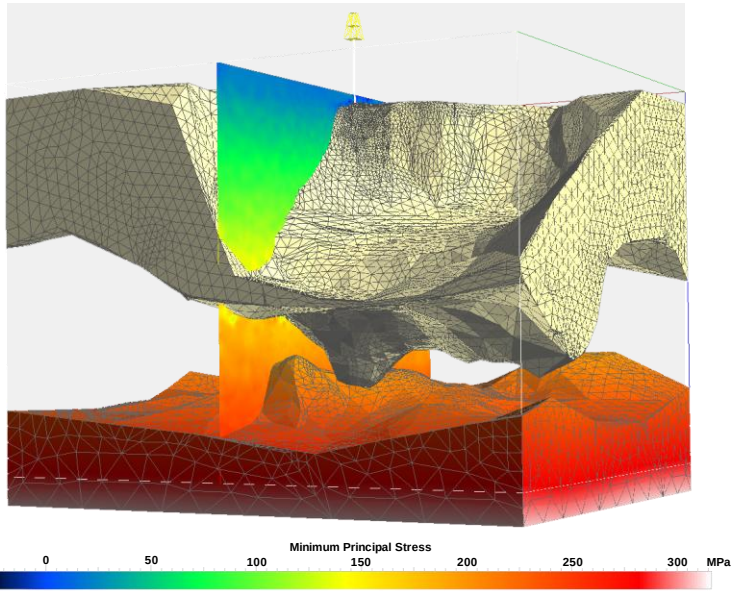

a)

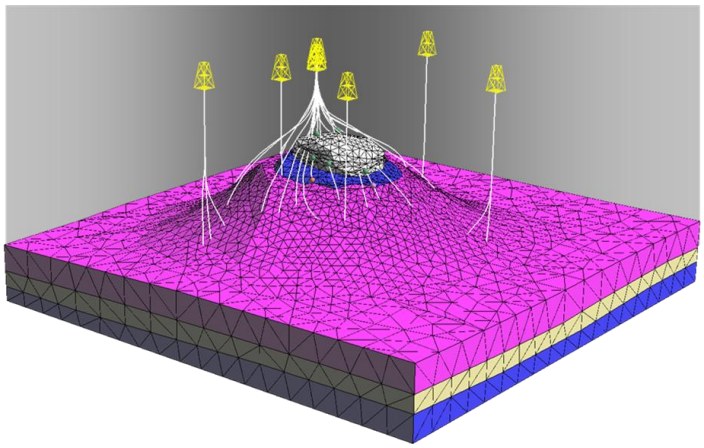

b)

Figure 4: a) FE mesh of Gulf of Mexico salt sheet. Note the fine mesh near the wellbore which coarsens to the outside of the model. The cross section shows the minimum principal stress field. b) FE mesh of a field around a salt dome. Note how the mesh refines near the salt structure to obtain the maximum resolution.

2.5 Mechanical Property and Pore Pressure Population

The mechanical properties are transferred from the 3D cubes to each node in the FE model using user-defined fields. The material properties in the mesh are made dependent on these field variables. From these nodes, each integration point calculates its material behavior during the FE analysis.

Because the baseline model of the geological (property) model and the FE mesh is the same structural model, the mapping generates the same variations and heterogeneity in the FE model as in the original property model. This guarantees that the property distribution in the FE model reflects the true lateral and depth variability of these parameters. This is of importance for the model to capture the changes in mechanical behavior due to the changes in geology throughout the 3D volume.

Also the pore pressure is mapped from the 3D pore pressure cube on each node in the FE mesh. In the presented models, the pore pressure boundary conditions are applied for each node, and kept constant during the analysis. However, the pore pressure boundary conditions could also be varied in time using reservoir simulator results, if available (i.e., Castillo et al., 2010).

The outside boundaries are given displacement boundary conditions of zero in x, y, and z direction. A distributed load at the sea floor is applied to simulate the load of the water column. This load is depth dependent and normal to the surface of the water base.

2.6 FE analysis steps

The finite element analyses are performed using the implicit solver of Abaqus/Standard. The simulations calculate the stress perturbation due to the presence of the salt body. The starting point for such a simulation is the initial (1D and unperturbed) stress state. The unperturbed stress state is not in equilibrium with the model and will be the reason that the model deforms to find the equilibrium state. These deformations must be minimal to avoid large changes in the geometry, and to avoid generation of unrealistic near surface stresses. To avoid these problems, a two tier approach is used which is a modification of the method described by Ellis (2006):

- In the first tier, we apply a rough initial stress field to the FE model. This model is run for a geostatic step which only calculates the elastic equilibrium. During this single step, gravity is applied to the whole model and the vertical stress is calculated. For every element in the FE model, the full stress tensor is calculated using the vertical stress combined with the knowledge of Azi_{SH} and the effective stress ratios for S_{hmin} and S_{Hmax}. These stresses are used as the initial stress conditions in the second tier.
- In the second tier, the original boundary conditions and the undeformed mesh shape are used together with the initial stresses calculated in the first tier. The calculation of the stress perturbation is done in two steps:
    - Geostatic analysis to calculate the elastic equilibrium of the model,
    - Creep step to model the salt creep.

In the second step, the differential stresses in the salt body cause salt creep which, in turn, reduces these differential stresses. This step is chosen of a long enough period to reduce the differential stresses within the salt structure to a level approximately equal to the magnitude of

measured/expected values (see discussion). During the creep step, the model stays in elastic equilibrium.

2.7 Model Size and Hardware

The models described in this paper consist of up to 450,000 2nd order tetrahedron elements (C3D10M & C3D10MP), resulting in calculations with up to $4 \cdot 10^6$ degrees of freedom. The creep part of the simulation needs many increments (up to 120) which results into relatively large problem. To be able to handle this size of models we perform all our calculations on a Windows HPC cluster with 5 nodes, with 16GB internal memory and 4 cores per node (20 cores and 80 GB RAM in total). On this cluster a typical calculation runs up to 6 days. However, the use of the newly introduced iterative solver in Abaqus 6.10 can significantly reduce this calculation time.

2.8 Visualization of the results

The results of the finite element model are exported to JewelSuite for visualization. JewelSuite is used as visualization tool to allow for direct comparison with well based data. The following parameters are exported from the finite element system: the full 3D stress tensor, the pore pressure, the effective stress ratio (as defined in equation 4), and all 3 principal stresses.

$$ESR = \frac{S_3 - P_p}{S_1 - P_p} \qquad \text{Eq. 4}$$

The results for each node are extracted in Abaqus/CAE using a Python script. Since the JewelSuite software knows the connectivity of the nodes it can displays the results in 3D. The software allows the display of multiple arbitrary cross sections to QA/QC the results. The final results are mapped from the FE Mesh onto a well path for direct comparison with the well data. The same approach is used for a wellbore stability study where the full 3D stress tensor is mapped on the well path resulting in a wellbore stability study based on stresses with the most realistic magnitudes and orientations.

3. Results

The main result of the finite element analysis is that the full 3D stress-tensor describing the magnitudes and orientations of all three principal stresses for every position in the model is obtained.

Extracting stress profiles for the regions remote to the salt structure in the model shows that these profiles follow the original ESR and pore pressure profiles. Moreover, the azimuth of the maximum horizontal stress along these paths is the same as the original applied $AziS_H$ derived from far field stresses. The effective stresses at the water base are close to 0 MPa, with a sporadic maximum difference of around 1 MPa. The orientations of the principal stresses at the water base – sediment interface are either parallel or perpendicular to this interface.

The results of the FE model shows that differential stresses in the salt body are up to 2-3 MPa, which corresponds to an effective stress ratio of approximately 1.0. The principal stresses near the salt-clastic interface are all either parallel or perpendicular as one would expect from the fact that the creeping salt acts like a free surface (Figure 5).

The effective stress ratio in the clastic sediments depends strongly on the position with respect to the salt body as well as the shape of the salt structure. At the horizontal interface at the base of the salt sheet in the GOM models, the influence of the salt body is not significant. But at a convex salt-clastic interface (e.g., a downward bulge of the salt layer), the minimum principal effective stress and the stress ratio are reduced drastically (Figure 6). In contrast, at concave salt-clastic interface the minimum principal stress and effective stress ratio are increased.

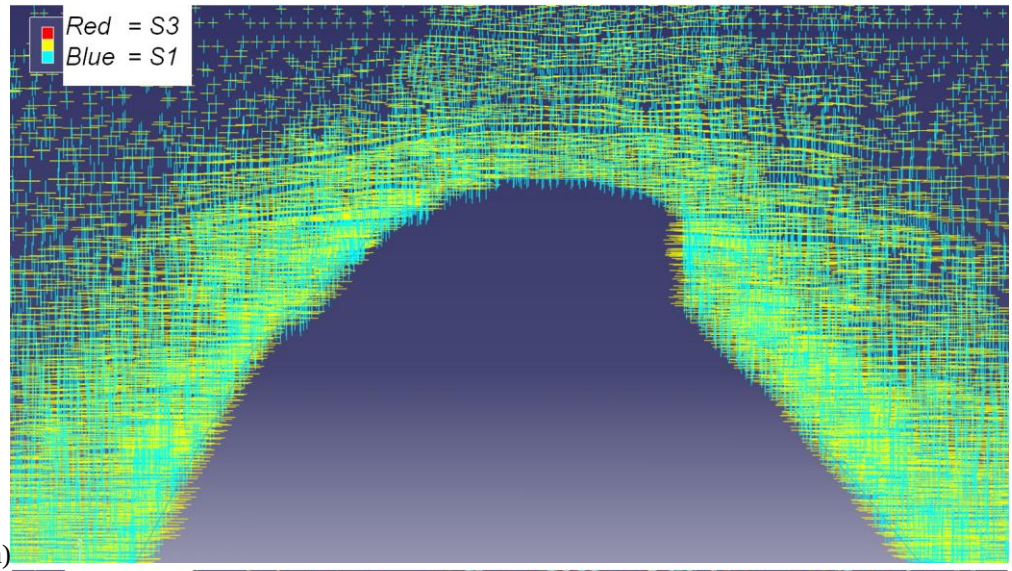

a)

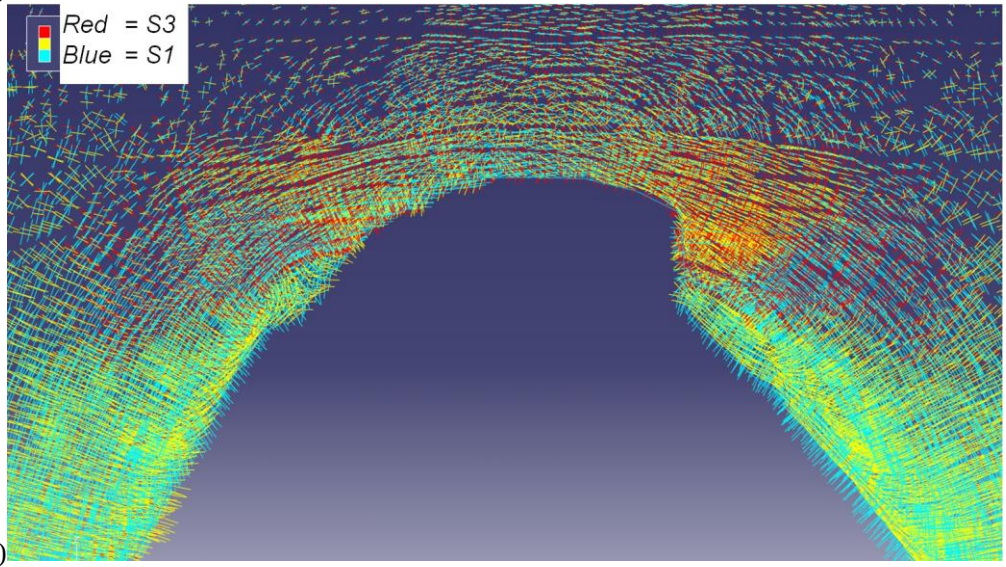

b)

Figure 5: Cross section through the model with results for the salt dome in the middle removed for visual purposes. In the initial state of the analysis (a), the

vertical stress is a principal stress. At the final stress state (b), the salt creep has reduced the differential stress to 2-3 MPa. Note that all principal stresses have rotated to either parallel or perpendicular to the salt-clastic interface.

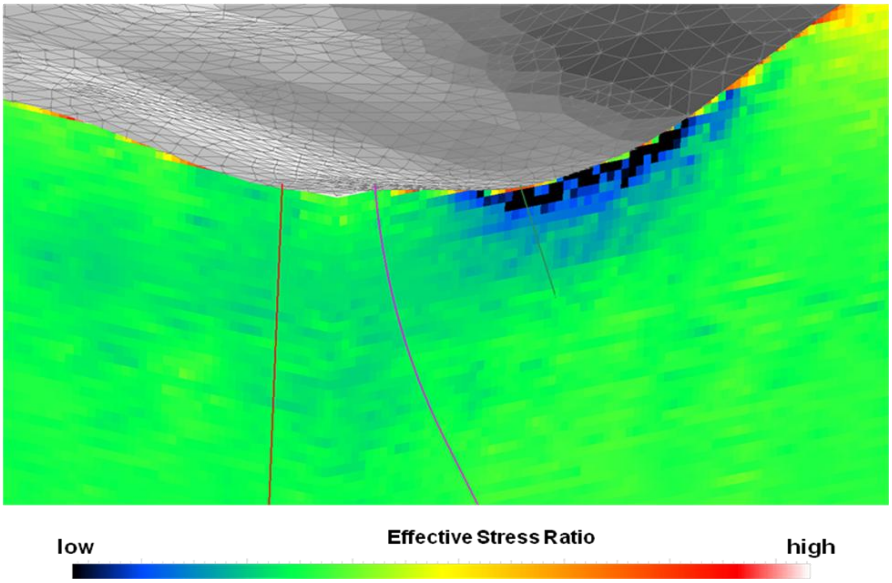

Figure 6: Effective stress ratio below a salt sheet. The drilling experience in the red well showed no major changes in fracture gradient, while the green well encountered major loss problem at the salt exit.

4. Discussion

4.1 Verification of results

After the first initial elastic step, differential stresses of significant magnitude are found in the salt body. The magnitude of these differential stresses decreases due to salt creep in the second step of the model. The creep step should be chosen long enough to create geologically realistic stress states in the salt. The 2-3 MPa differential stress predicted by our models is in agreement with subgrainsize piezometery performed on typical Gulf of Mexico salts (Digs et al., 1997).

The second verification is to check if the stresses at the salt-clastic interface are either parallel or perpendicular to this interface. Figure 5 shows a case study example where we compare the initial stress state, where the vertical stress is a principal stress, with the final stress state, where the stress are in equilibrium with the creeping salt body. This verification step should be performed in every study involving salt to check if the rotations are physically correct and not a result of numerical problems or mode set-up.

The final verification is to check measured S_{hmin} values (e.g., LOT) with the modeled stresses. In one case study with a salt dome, we have a list of measured S_{hmin} values. To verify to correctness

of our results, we have compared the reported S_{hmin} values with the simulated minimum principal stresses (Figure 7). The comparison shows that we have a good fit between the FE results and most of the S_{hmin} measurements, however in some cases, the minimum principal stress predictions based on our model does not agree well with the measured values. In another case study in the Gulf of Mexico (shown in Figure 6), we have both LOT results and some drilling experience. Both the LOT and the occurrence of lost circulation were predicted within 5%, which is a remarkably good result.

The verification process has shown in many studies that the predicted minimum stress is near the minimum stress measured in the field. This positive match shows that the predicted stresses are robust and that the stresses predicted by the FE model can be used in pre-drill models.

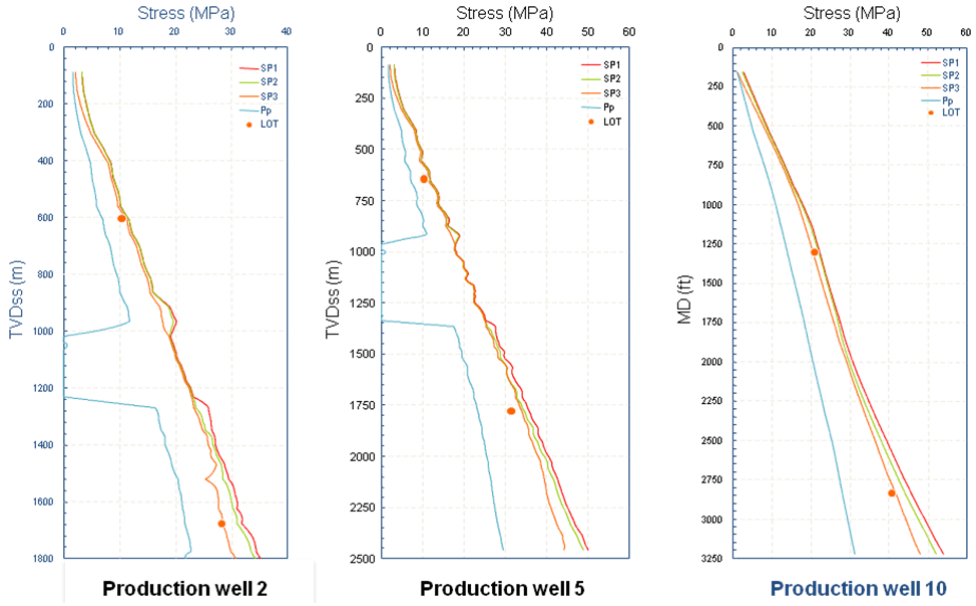

Figure 7: Comparison between stresses calculated in the FE model (lines) and actual LOT (orange dots).

4.2 What is the influence of the salt geometry?

The results of our models show that the stress magnitudes and orientation is strongly dependent on the 3D geometry of the salt – clastic interface and the 3D position to the salt body. This means that the shape of the salt body should be as well defined as possible. The software used to create the surfaces describing the salt structure (JewelSuite in our case) should be able to handle most complex structures without limitations. Software which allows only 2D gridding which can't create overhanging structures is too limited to be used in this kind of modeling.

The strong shape dependence means that an uncertainty in picking the shape of the interface can have a large effect on the results. Also the time-depth conversion performed in the first phases of the study has a distinct effect on the predicted salt-exit depth. An unreliable interval velocity can result in a significant depth shift. As a consequence, significant changes in fracture gradient (Figure 6) can be encountered on a shallower depth than anticipated, thus, resulting in significant losses and related well control problems.

The models show that the stress perturbations due to the salt-clastic interface geometry are very case specific. The general statements made in the results section are valid, but a case-specific model is needed to predict the extent and to quantify the magnitude of the stress perturbations.

Comparing our models with studies that use only 2D profiles show that to estimate the correct principal stress magnitudes, a full 3D model is needed, because different 2D cross sections can result in different values of principal stresses for the same position at the intersections (e.g., Fredrich et al., 2007)

4.3 Application of Results

Because the FE results are imported into a 3D geological modeling package, we can directly use these result together with other available information of the field being modeled. For wellbore stability purposes, we extract the results along a well path. This output along the well path only shows small extrapolation errors showing the benefits of the optimized meshing technique. The stresses along the well path are combined with material properties such as UCS and can be used to perform a wellbore stability analyses in dedicated software.

5. Conclusions

- Baker Hughes RDS has established a workflow that derives a three-dimensional finite-element mesh from a structural field model. This model is populated with densities and elastic properties from a 3D model of these data and thus, incorporates regional and vertical variability of these parameters.
- The finite-element simulations realistically and physically correctly predict the stresses field around a salt structure.
- Case studies have verified the predicted fracture gradient below the salt within 5%.
- The simulation results can be directly transferred into wellbore stability software (e.g., GMI-WellCheck). This workflow provides an optimized input for wellbore stability prediction studies for high-cost wells close to salt structures.
- The same workflow in combination with reservoir simulation results can be applied for the prediction of reservoir compaction and surface subsidence.

6. References

Bowers, G. L. “Pore Pressure Estimation From Velocity Data: Accounting For Overpressure Mechanisms Besides Undercompaction”, IADC/SPE, Drilling Conference, Dallas, TX, February 15-18, 1994, IADC/SPE 27488: 515 – 530, 1994.

Brudy, M., M. D. Zoback, K. Fuchs, F. Rummel, and J. Baumgärtner. “Estimation of the complete stress tensor to 8 km depth in the KTB scientific drill holes: implications for crustal strength” Journal Geophysical Research, v.102, no.8: 18,453-18,475, 1997.

Brudy, M. and H. Kjørholt. “Stress orientation on the Norwegian continental shelf derived from borehole failures observed in high-resolution borehole imaging logs”, Tectonophysics, v.337: 65-84, 2001.

Castagna, J.P. “Relationships Between Compressional-Wave and Shear-Wave Velocities in Clastic Silicate Rocks”, Geophysics, Vol. 50, No. 4: 571-581, 1985.

Castillo, D., van der Zee, W. and Brudy, M. “3D geomechanical applications for drilling and evaluating reservoirs”, SPE news, 132, 26-29, 2010.

Diggs T. N. Urai J. L. Carter N. L. “Rate of flow in Salt sheets, Gulf of Mexico: Quantifying the risk of casing damage in subsalt plays”, EUG 9, Strasbourg. Terra Nova, 9, Abstract Supplement No 1: 172, 1997.

Ellis, S. “Attaining geostatic equilibrium and initial stress states: crustal faulting experiments using Abaqus”, Geoqus Workshop, Bochum, 2006.

Fredrich, J.T., Engler, B.P., Smith, J.A., Onyia, E.C. and Tolman, D.N. “Predrill Estimation of Subsalt Fracture Gradient: Analysis of the Spa Prospect to Validate Nonlinear Finite Element Stress Analyses”, SPE/IADC 105763, 2007.

Gaarenstroom, L., Tromp, R.A., de Jong, M.C. & Brandenburg, A.M. “Overpressures in the Central North Sea: implications for trap integrity and drilling safety”, In: Parker, J.R. (ed.) Petroleum Geology of Northwest Europe. Proceedings of the 4th Conference. The Geological Society, London: 1305–1313, 1993.

Moos, D. and M.D. Zoback. “Utilization of observations of well bore failure to constrain the orientation and magnitude of crustal stresses: Application to continental, Deep Sea Drilling Project and ocean drilling program boreholes”, Journal Geophysical Research, v.95: 9305-9325, 1990.

Moos, D. et al. “Quantitative Risk Assessment Applied to Pre-drill Pore Pressure, Sealing Potential, and Mud Window Predictions from Seismic Data”, Gulf Rocks 2004, 6th North America Rock Mechanics Symposium (NARMS), Jun. 5-9, 2004, pp. 1-8, 10.

Raaen, A.M., and M. Brudy. “Pump-in/Flowback Tests Reduce the Estimate of Horizontal In Situ Stress Significantly”, SPE 71367, 2001.

Yu, Z., Lerche, I., and Lowrie, A. “Thermal Impact of Salt: Simulation of Thermal Anomalies in the Gulf of Mexico”, Pageoph, 138(2), 1992.

Ward, C.D., Coqhill, K., and BrousssrrL, M.D. “The Application of Petrophysical Data to Improve Pore and Fracture Pressure Determination in North Sea Central Graben HPHT Wells”, SPE 28297: 53-68, 1992.

Willson, S.M., Fossum, A.F., and Fredrich, J.T. “Assessment of Salt Loading on Well Casings”, SPE Drilling & Completion, 18(1), 13-21.

Zoback, M.D., Barton, C.A., Brudy, M., Castillo, D.A., Finkbeiner, T., Grollimund, B.R., Moos, D.B., Peska, P., Ward, C. D., Wiprut, D.J.” Determination of stress orientation and magnitude in deep wells”, International Journal of Rock Mechanics and Mining Sciences, 40 (7): 1049-1076, 2003.

Zoback, M.D. “Reservoir Geomechanics: Earth Stress and Rock Mechanics Applied to Exploration, Production and Wellbore Stability”, Cambridge Press, Cambridge Press, 449 pp. , 2007.

7. Acknowledgement

We like to thank Devon Energy Corporation and BP Exploration Operating Company Limited and its partners for permission to publish figures contained in this document. The authors like to thank Baker Hughes Inc. management for permission to publish this article.